Published in final edited form as:
Circulation. 2013 August 6; 128(6): 632–642. doi:10.1161/CIRCULATIONAHA.113.002714.

SREBP2 Activation of NLRP3 Inflammasome in Endothelium Mediates Hemodynamic-Induced Atherosclerosis Susceptibility

Han Xiao, MD, PhD[1,2], **Min Lu, MD, PhD**[3], **Ting Yang Lin, MS**[1], **Zhen Chen, PhD**[1,3], **Gang Chen, MD**[4], **Wei-Chi Wang, PhD**[5], **Traci Marin, MS**[1], **Tzu-pin Shentu, PhD**[1], **Liang Wen, PhD**[1], **Brendan Gongol, MS**[1], **Wei Sun, MD**[1], **Xiao Liang, MD, PhD**[6], **Ju Chen, PhD**[3], **Hsien-Da Huang, PhD**[5], **Joao H.F. Pedra, PhD**[4], **David A. Johnson, PhD**[1], and **John Y-J. Shyy, PhD**[1,3,6]

[1]Division of Biomedical Sciences, University of California, Riverside, CA

[2]Institute of Vascular Medicine of Peking University Third Hospital, Beijing, China

[3]Department of Medicine, University of California, San Diego, La Jolla, CA

[4]Center for Disease Vector Research and Department of Entomology, University of California, Riverside, CA

[5]Department of Biological Science and Technology, Institute of Bioinformatics and Systems Biology, National Chiao Tung University, HsinChu, Taiwan

[6]Cardiovascular Research Center, Medical School, Xi'an Jiaotong University, Xi'an, China

Abstract

Background—The molecular basis for the focal nature of atherosclerotic lesions is poorly understood. Here, we explored whether disturbed flow patterns activate an innate immune response to form the NLRP3 inflammasome scaffold in vascular endothelial cells (ECs) via sterol regulatory element binding protein 2 (SREBP2).

Methods and Results—Oscillatory flow activates SREBP2 and induces NLRP3 inflammasome in ECs. The underlying mechanisms involve SREBP2 transactivating NADPH oxidase 2 (NOX2) and NLRP3. Consistently, SREBP2, NOX2, and NLRP3 levels were elevated in atheroprone areas of mouse aortas, suggesting that the SREBP2-activated NLRP3 inflammasome causes functionally disturbed endothelium with increased inflammation. Mimicking the effect of atheroprone flow, EC-specific overexpression of the activated form of SREBP2 synergized with hyperlipidemia to increase atherosclerosis in the atheroresistant areas of mouse aortas.

Conclusions—Atheroprone flow induces NLRP3 inflammasome in endothelium through SREBP2 activation. This increased innate immunity in endothelium synergizes with hyperlipidemia to cause topographic distribution of atherosclerotic lesions.

Correspondence: John Y-J. Shyy, PhD, Department of Medicine/Division of Cardiology, University of California, San Diego, 9500 Gilman Drive, La Jolla, CA 92093, Phone: 858-534-3736, Fax: 858-822-3027, jshyy@ucsd.edu.

Conflict of Interest Disclosures: None.

Keywords

shear stress; endothelial cell; atherosclerosis; inflammasome; SREBP

Introduction

Atherosclerosis preferentially develops at branches and curvatures in the arterial tree. Cardiovascular risk factors such as hyperlipidemia, smoking, and hypertension increase the prevalence and severity of lesions in these atheroprone regions[1]. At the cellular and molecular levels, disturbed-flow patterns with low shear stress such as those found at vascular branches and curvatures increase the expression of genes, e.g., interleukin 1β (IL-1β), NADPH oxidase (NOX), to promote inflammatory and oxidative stresses in vascular endothelial cells (ECs)[2, 3]. Such hemodynamic-induced functionally disturbed endothelium predisposes localized areas to become atherogenic, with ensuing monocyte recruitment and foam cell formation. Although extensive studies have revealed EC gene expression profiles associated with the atheroprone flow patterns, the key molecular events linking mechanical stimuli to atherogenic responses remain undetermined.

Sterol regulatory element binding protein 2 (SREBP2) plays a canonical role in cholesterol homeostasis by its transcriptional regulation of molecules involved in cholesterol biosynthesis and low density lipoprotein (LDL) uptake[4]. Cholesterol depletion leads to increased expression of SREBP2 along with its intronic microRNA-33 (miR-33), which replenishes cellular cholesterol by inducing genes that encode proteins such as 3-hydroxy-3-methyl-glutaryl (HMG)-CoA reductase and LDL receptor (LDLR) and suppressing the ATP-binding cassette transporter 1 (ABCA1)[5, 6]. Conversely, elevated levels of sterols suppress SREBP expression, thereby lowering cellular cholesterol levels. This homeostasis might be disrupted by atheroprone flow patterns, which induce sustained activation of SREBP1 and perturbation of EC function[7].

The connection between hemodynamic-induced endothelial dysfunction and inflammatory and oxidative stresses is poorly understood. However, aberrant lipid metabolism, unbalanced redox states, and innate immunity in phagocytes are linked through NLRP3 inflammasome with subsequent cleavage and activation of IL-1 family proteins[8]. Moreover, cholesterol crystals activate the NLRP3 inflammasome and increase the secretion of mature IL-1β in monocyte/macrophages[9, 10]. LDLR-deficient mice receiving bone-marrow-derived cells lacking NLRP3, ASC, or IL-1α/β were resistant to the development of diet-induced atherosclerosis[9]. Alone, systemic activation of NLRP3 inflammasome in macrophages does not explain the preferential localization of atherosclerosis in the arterial tree.

Disturbed flow can activate NOX and induce reactive oxygen species (ROS)[11]. This raises the possibility that inflammasome is involved in oxidative stress in ECs. Additionally, a recent report of minute cholesterol crystals appearing early in atherosclerotic lesions[9] suggests a linkage between hemodynamic stimuli, SREBP2 activation, and NLRP3 inflammasome in ECs, all linked to atherosclerosis. Using *in vitro* and *in vivo* approaches, we report here that the atheroprone flow-induced endothelial inflammation and oxidative stress are mediated through SREBP2-elicited NLRP3 inflammasome. Our findings reinforce a primary role of EC innate immunity in the etiology of atherosclerosis.

Materials and Methods

Antibodies and Reagents

Anti-SREBP2 antibody was from BD Transduction Laboratory and Abcam; anti-IL-1β, anti-caspase-1, anti-α-tubulin, horseradish peroxide-conjugated anti-rabbit and anti-mouse antibodies were from Cell Signaling Technology; anti-ABCG1, anti-NLRP3, anti-NOX2 antibodies were from Abcam; anti-ABCA1 antibody was from Millipore; and anti-ASC antibody was from Enzo Life Science. The caspase-1 inhibitor Z-YVAD-FMK was from Biovision. 25-hydroxycholesterol (25-HC) and methyl-beta-cyclodextrin (MβCD) were from Sigma.

Cell Culture

Human umbilical vein ECs (HUVECs) were cultured in medium M199 (Gibco) supplemented with 15% FBS (Omega), 3 ng/mL β-EC growth factor, 4 U/mL heparin, and 100 U/mL penicillin-streptomycin. Total cholesterol was measured by use of the Infinity total cholesterol kit (Thermo Scientific). Caspase-1 activity was measured with the use of Caspase-1/ICE Colorimetric Assay Kit (R&D Systems). Primary mouse lung ECs were isolated as described[12].

Shear Stress Experiments

A circulating flow system was used to impose shear stress on confluent monolayers of cells seeded on glass slides as described[13]. A reciprocating syringe pump connected to the circulating system introduced a sinusoidal (1 Hz) component onto the shear stress. The atheroprotective pulsatile shear flow (PS) or atheroprone oscillatory shear flow (OS) generated shear stresses of 12 ± 4 dyn/cm^2 or 1 ± 4 dyn/cm^2, respectively. The flow system was enclosed in a chamber held at 37°C and ventilated with 95% humidified air plus 5% CO_2.

siRNA Knockdown

HUVECs at 50–70% confluence were transfected with SREBP2 siRNA, NLRP3 siRNA, ASC siRNA, NOX2 siRNA, or control siRNA at 20 nM with Lipofectamine 2000 RNAi Max (Invitrogen). Experiments were performed with these cells at 48 hr post-transfection.

Adenovirus Construction and Infection

Recombinant adenovirus encoding the mature form of SREBP2, i.e., Ad-HA-SREBP2(N) was created, amplified, and titrated as reported previously[14]. For adenovirus infection, the virus mixture was added to 70% confluent cultured HUVECs and incubated for 12 hr. Ad-null was an infection control. The infected cells were then incubated in fresh growth medium for 24 hr before RNA or protein extraction.

Binding Sites Prediction

The potential SREBP2 binding sites on selected human and mouse genes were predicted using position weight matrix (PWM) algorithm from TRANSFAC[15] to scan the promoter regions of the genes. The promoter regions were defined as −3000~ 500 from the transcriptional start site of the gene.

Chromatin Immunoprecipitation (ChIP) Assay

ChIP assays were performed with standard protocols[16] using antibodies for SREBP2 (BD Transduction Laboratory) and mouse IgG (Cell Signaling).

EC-SREBP2(N) Transgenic Mice

Animal experimental protocols were approved by the Institutional Animal Care and Use Committee of the University of California, Riverside. The creation of the EC-SREBP2(N)-Tg mouse model is described in Supplemental information. Littermates carrying $ApoE^{-/-}$ or EC-$SREBP2(N)^{+/+}ApoE^{-/-}$ genotypes were generated by crossing EC-SREBP2(N)-Tg mice and $ApoE^{-/-}$ mice. All mice were housed in colony cages with a 14-hr light/10-hr dark cycle and fed Rodent Diet 5001 (PMI Nutrition International) *ad libitum* unless otherwise indicated. Eight-week old male EC-$SREBP2(N)^{+/+}ApoE^{-/-}$ and their male EC-$SREBP2(N)^{-/-}ApoE^{-/-}$ littermates were fed a high-fat, high-cholesterol diet containing 15% fat, 1.25% cholesterol, and 0.5% sodium cholate (Harlan Teklad) *ad libitum*. Eight weeks after the diet treatment, all mice were sacrificed. In addition, 24-week-old male EC-$SREBP2(N)^{+/+}ApoE^{-/-}$ and their male EC-$SREBP2(N)^{-/-}ApoE^{-/-}$ littermates were fed normal chow. Mouse aortas were isolated to assess the extent and distribution of lesions by Oil Red O staining[17]. Lesion area was measured using Image Pro Plus 6.0 (Media Cybernetics) and expressed as a percentage of the total area of aorta. Plasma levels of total cholesterol, HDL cholesterol, and triglycerides were determined using assay kits from Wako Pure Chemicals (Tokyo, Japan).

Statistical Analysis

Data are expressed as means ± SEM (n = 3 unless otherwise noted). In parametric data, Student's *t* test or ANOVA was used to analyze the differences among groups if data were determined to be normal distribution. For non-parametric data, Mann-Whitney U test with exact method was used to analyze the differences between two groups. $P<0.05$ was considered statistically significant.

Results

Co-Induction of SREBP2 and miR-33 in ECs by OS

Initially, we examined the effects of PS and OS on the expression of SREBP2 in ECs. Imposition of OS, but not PS, activated SREBP2, as evidenced by the increased level of the mature form of SREBP2, namely SREBP2(N), and SREBP2 mRNA (Figure 1A and 1B). Given that miR-33 is intronic with SREBP-2, OS elevated the level of miR-33 as well (Figure 1B). Additionally, the expression of SREBP2-targeted genes, ie, HMG-CoA reductase, HMG-CoA synthase, squalene synthase, and LDLR was higher with OS than PS (Figure 1C). The miR-33-targeted ABCA1, but not ABCG1, was down-regulated at both transcriptional and translational levels (Figure 1D & 1E). Thus, OS increased the expression of genes involved in cholesterol synthesis and uptake while decreasing ABCA1, which is involved in cholesterol efflux. In line with these changes, the cholesterol content of HUVECs was greater with OS than PS (Figure 1F). One possible mechanism for OS induction of SREBP2 is that the action of OS is secondary to sterol depletion. Consequently, we examined whether sterol replenishment with 25-HC blocks the effect of OS on SREBP2 activation. While 25-HC and MβCD reduced and increased SREBP activation in HUVECs, respectively, incubation of 25-HC had little effect on OS-induced SREBP2 expression (Figure 1G). Interestingly, overexpression of the mature form of SREBP2, ie, SREBP2(N) or pre-miR33, increased the cholesterol content (Figure S1A and S1B). However, siRNA knockdown of SREBP2, but not miR-33, abolished OS-induced cholesterol accumulation (Figure S1C, D). Consequently, we focused on the role of SREBP2 in OS-disturbed endothelial functions.

OS Induces NLRP3 Inflammasome in ECs via SREBP2

The atheroprone nature of OS is largely due to its imposition of inflammatory and oxidative stresses on ECs[18]. Because SREBP1a induces caspase-1-activated NLRP3 inflammasome in macrophages, resulting in cleavage and secretion of IL-1 family cytokines[19], we investigated whether OS induces inflammasome in ECs. The levels of cleaved caspase-1 and IL-1β were greater in ECs with OS than PS (Figure 2A). Because OS induced SREBP2 maturation, we explored whether SREBP2(N) overexpression mimics OS to induce inflammasome in ECs. As expected, increased cleavage of caspase-1 and IL-1β was found in ECs infected with Ad-SREBP2(N) encoding SREBP2(N) (Figure 2B). Consistent with this finding, ectopic expression of SREBP2(N) increased caspase-1 activity in ECs (Figure 2C). With siRNA knockdown of endogenous SREBP2, OS-induced cleavage of caspase-1 or IL-1β was reduced (Figure 2D). Similar results were found when the inflammasome components NLRP3 and ASC were knocked down (Figure 2E and 2F). Together, these results suggest that SREBP2 mediates OS-induced NLRP3 inflammasome in ECs.

SREBP2 Upregulates NOX2 with Increased ROS Production

We then investigated the underlying mechanism by which SREBP2 regulates the OS-induced inflammasome in ECs. ROS level is increased by NLRP3 activators such as asbestos and silica[20] and increased ROS are secondary messengers essential for inducing NLRP3 inflammasome[20, 21]. Given that OS is known to increase ROS production[22], we examined SREBP2 augmentation in relation to ROS production. The intracellular level of ROS increased in ECs infected with Ad-SREBP2(N) encoding the mature form of SREBP2 (Figure 3A). To assess the source of increased level of ROS in ECs overexpressing SREBP2(N), we monitored ROS-generating mitochondria using MitoSOX, a selective mitochondrial superoxide indicator. Rotenone, the complex I inhibitor, greatly increased mitochondrial ROS production, but Ad-SREBP2(N) overexpression was without effect (Figure 3B). Therefore, the increased ROS production caused by SREBP2 activation probably did not originate from mitochondria. Bioinformatics predicted the presence of 3 sterol regulatory elements (SREs) in the promoter region of the human *NOX2* gene (−2381/−2367, −867/−861, and −674/668 bp) (Figure 3C). Consistent with this prediction, the levels of NOX2 mRNA and protein increased in Ad-SREBP2(N)-infected HUVECs as well as in ECs isolated from transgenic mice overexpressing SREBP2(N) in endothelium [EC-SREBP2(N)-Tg] (Figure 3D–3F). Of note, the levels of other NADPH oxidase subunits (except NOX1) were not significantly increased in these cells (Figure S2). ChIP assay demonstrated an increase in the binding of SREBP2 to the 3 SREs containing the consensus sequence of CACC(T)CCA (Figure 3G). To investigate whether SREBP2 is required for OS-induced NOX2, we knocked down SREBP2 and found that the OS-induced NOX2 was partially suppressed (Figure 3H). Furthermore, NOX2 knockdown inhibited the OS-induced caspase-1 and IL-1β cleavage (Figure 3I). Similar inhibitory effect was found in $NOX2^{-/-}$ mouse embryonic fibroblasts (Figure S3). These results suggest that the SREBP2-transactivated NOX2 is required for OS-induced inflammasome in ECs.

SREBP2 Up-regulates NLRP3 Expression

Bioinformatics also predicted the presence of an SRE located at −1379/−1368 bp in the promoter region of the *NLRP3* gene (Figure 4A). As expected, NLRP3 expression was increased in Ad-SREBP2(N)-infected HUVECs (Figure 4B and 4C) and ECs isolated from EC-SREBP2(N)-Tg mice (Figure 4D). ChIP assays demonstrated an increase in the binding of SREBP2 to SRE containing the consensus sequence CCGCCACCACAC (Figure 4E). To investigate whether SREBP2 is required for OS-induced NLRP3 expression, we knocked down SREBP2. Accordingly, the level of NLRP3 responding to OS was decreased (Figure 4F). Therefore, the OS-activated SREBP2 transactivates NLRP3 in ECs.

SREBP2(N) Overexpression Enhances Endothelial Inflammation

IL-1β stimulates the expression of chemokines, eg, monocyte chemoattractant protein 1 (MCP-1), and adhesion molecules, eg, vascular cell adhesion molecule 1 (VCAM-1), E-selectin, in ECs, which enhances leukocyte-endothelial interactions. In agreement with increased IL-1β secretion via SREBP2-augmented inflammasome, SREBP2(N) overexpression increased the mRNA levels of MCP-1, VCAM-1, and E-selectin (Figure 5A). An increased expression of MCP-1 and adhesion molecules was also found in ECs isolated from EC-SREBP2(N)-Tg mice, when compared with wild-type littermates (Figure 5B). The SREBP2(N)-induced inflammation in ECs was associated with increased monocyte association, which was attenuated with caspase-1 inhibitor or NOX2 or NLPR3 siRNA knockdown (Figure 5C and 5D). Thus, NLRP3 inflammasome induced by OS via SREBP2 is functionally linked to endothelial pro-inflammatory responses.

SREBP2-NOX2-Inflammasome Activation in Atheroprone Regions of the Mouse Aorta

We next investigated whether the differential regulation of SREBP2 by PS and OS in ECs cultured in the flow channel also translated to a functional or functionally disturbed endothelium in atheroprotective versus atheroprone regions in the mouse arterial tree. As shown in Figure 6A and 6B, the activation of NLRP3 inflammasome was evident in the aortic arch, where the endothelium is predominantly exposed to disturbed flow[23]. As expected, the levels of the cleaved caspase-1 and IL-1β, ie, IL-1β p17, were higher in the aortic arch than thoracic aorta (Figure 6B). Consistent with this observation, the expression of IL-1β-regulated genes, ie, MCP-1, VCAM-1, intercellular adhesion molecule 1 (ICAM-1), and E-selectin, were all increased in the aortic arch (Figure 6A). In addition, we separated intima (endothelium) from media and adventitia of thoracic aorta and aortic arch of C57BL/6 mice. As illustrated in Fig. 6C, the expression level of SREBP2, NOX2, and NLRP3 in the isolated endothelium in aortic arch was higher than those in thoracic aorta. Importantly, no differences were found between thoracic aorta and aortic arch in tissues containing media and adventitia. Higher level of NLRP3, NOX2, and SREBP2 in the aortic arch was also verified by *in situ* hybridization (Figure S4). Thus, the NLPR3 inflammasome is activated in the endothelium of atheroprone region of the arterial tree *in vivo*.

EC-specific SREBP2(N) overexpression mimicking OS induction of SREBP2 should render the thoracic aorta of EC-SREBP2(N)-Tg mice to become “atheroprone”. As expected, activation of NLRP3 inflammasome and induction of chemoattractants and adhesion molecules were seen in these arterial segments as compared with corresponding areas in wild-type littermates (Figure 6D). SREBP2(N) overexpression also caused a functionally disturbed endothelium, as evidenced by impaired vasodilation responding to flow (Figure S5).

SREBP2(N) Overexpression in EC Predisposes Atherosclerosis

We introduced the ApoE-null background into EC-SREBP2(N)-Tg mice to investigate whether EC-specific overexpression of SREBP2(N) leads to atherogenesis in atheroprotective regions in $ApoE^{-/-}$/EC-SREBP2(N) mice. After 8 weeks of an atherogenic diet, the levels of total cholesterol and LDL were comparable between $ApoE^{-/-}$/EC-SREBP2(N) and their $ApoE^{-/-}$ littermates (Table 1). However, the mean lesion area in thoracic aortas was ~1.5-fold larger for $ApoE^{-/-}$/EC-SREBP2(N)-Tg than $ApoE^{-/-}$ mice (17.4 ± 1.7 vs. 11.5 ± 1.3%) (Figure 7A and 7C). The mean lesion area in the aortic arch was also larger for $ApoE^{-/-}$/EC-SREBP2(N) than $ApoE^{-/-}$ mice (47.7 ± 2.5% vs. 39.7 ± 3.1%). The order of lesion size was aortic arch of $ApoE^{-/-}$/EC-SREBP2(N) mice > aortic arch of $ApoE^{-/-}$ mice > thoracic aorta of $ApoE^{-/-}$/EC-SREBP2(N) mice > thoracic aorta of $ApoE^{-/-}$ mice. The total lesion area as a sum of aortic arch, thoracic aorta, plus abdominal aorta remained greater for $ApoE^{-/-}$/EC-SREBP2(N) than control littermates (22.5 ± 1.4%

vs. 18.2 ± 1.5%). These results demonstrate that local flow patterns synergize with other atherogenic factors, eg, hyperlipidemia, in the formation of atherosclerotic lesions. We also compared the lesion development in the two groups of animals fed normal chow for 24 weeks. As expected, the serum levels of total cholesterol and LDL were significantly lower with normal chow than an atherogenic diet (Table 1). Compared with the $ApoE^{-/-}$ littermates, $ApoE^{-/-}$/EC-SREBP2(N) mice showed more lesions in aortic arches, particularly the inner curvature of the arch and the orifices of the arch vessels (Figure 7B and 7D). Previous studies by others showed that these areas have elevated NFκB and VCAM-1 activation[23, 24]. Of note, with normal chow, lesion areas were marginal in the thoracic aortas of both $ApoE^{-/-}$/EC-SREBP2(N) and $ApoE^{-/-}$ mice, which reiterates the notion that hyperlipidemia synergizes with hemodynamic forces in the etiology of atherosclerosis.

Discussion

The “response-to-injury” hypothesis states that endothelial dysfunction precedes the development of atherosclerosis[25]. Much evidence suggests that atheroprone flow patterns in the conduit arteries are a determining factor of atherogenesis. Furthermore, the Pathological Determinants of Atherosclerosis in Youth (PDAY) study provides unequivocal evidence that cardiovascular risk factors (e.g., hyperlipidemia, smoking, and hypertension) exacerbate atherosclerosis in atheroprone areas in the human arterial tree[26, 27]. Here, we report that disturbed flow applied to ECs induced NLRP3 inflammasome via SREBP2 activation. Such SREBP2 activation of NLRP3 inflammasome is sufficient for functionally disturbed endothelium leading to atherogenesis as supported by mouse models harboring the EC-SREBP2(N) transgene. Differential development of atherosclerotic lesions in the aortic arch versus thoracic aorta in mice with or without EC-specific expression of SREBP2(N) and in the presence or absence of an atherogenic diet (Figure 7) provides a molecular basis for the hemodynamic-induced atherosclerosis susceptibility seen in human arterial tree. We reasoned that endothelial expression of SREBP2(N) mimicking the effect of disturbed flow synergizes with hyperlipidemia (caused by an $ApoE^{-/-}$ background together with an atherogenic diet) to accelerate atherosclerosis. The thesis is further supported by experiments using EC-SREBP2(N)-Tg or wild-type C57BL6 mice fed an atherogenic diet. Early atherosclerotic plaques developed in the aortic root of EC-SREBP2(N)-Tg but not control littermate mice (Figure S6 and Table 2). Thus, the translational relevance of this study is that the spatial localization and severity of atherosclerosis can depend on atheroprone flow coupled with cardiovascular risk factors via SREBP2(N)-induced NLRP3 inflammasome.

Clearly, IL-1β is a major atheroprone factor[28]. Atherosclerosis was decreased in several rodent models lacking IL-1β or type I IL-1 receptor[29, 30]. In contrast, mice deficient in IL-1 receptor antagonist show increased atherosclerosis[31]. Canakinumab, an anti-human IL-1β monoclonal antibody, is currently used in the Canakinumab Anti-inflammatory Thrombosis Outcomes Study (CANTOS) to assess the efficacy of anti-IL-1β in reducing cardiovascular events[32]. The anti-atherosclerosis effect resulting from IL-1β antagonism should involve the inhibition of NLRP3 inflammasome in the endothelium and should to be experimentally verified. Undoubtedly, NLRP3 inflammasome in monocyte/macrophage is important for atherosclerosis, as suggested by transplantation experiments with bone marrow deficient in NLRP3, ASC, or IL-1α/β[9]. However, this macrophage-associated mechanism would not contribute to functionally disturbed endothelium and ensuing atherosclerosis in our mouse models, because the SREBP2(N) transgene was expressed only in ECs and not in bone-marrow-derived macrophages (Figure S7).

Reconciling published literature with the current report, we propose that the disturbed flow-increased NLRP3 inflammasome in ECs and consequent production and secretion of IL-1β creates a focal gradient of inflammatory cytokines and chemoattractants. This flow-elicited pro-inflammatory milieu recruits sentinel cells (i.e., monocytes) and facilitates the retention and differentiation of monocytes in the sub-endothelial space. Indeed, atherosclerosis was found substantially lower in ApoE$^{-/-}$/IL-1β$^{-/-}$ than ApoE$^{-/-}$/IL-1β$^{+/+}$ thoracic aortas[30].

In macrophages, the SREBP2 co-induced miR-33a targets ABCA1, which impairs reverse cholesterol transport[5, 6]. An antigomir against miR-33 decreases atherosclerosis in LDLR-null mice, with concomitant increase in the level of HDL[33]. Inhibition of miR-33 also increases the level of HDL and lowers that of VLDL triglycerides in non-human primates[34]. In line with SREBP2 induction, OS-induced miR-33a targets ABCA1 in ECs (Figure 1). Given that cholesterol crystals are an inflammasome inducer[9], disturbed-flow patterns should increase the cholesterol level, which arguably synergizes with SREBP2 to activate NLPR3 inflammasome. Conversely, the atheroprotective flow patterns should induce liver X receptors and hence up-regulate ABCA1 to facilitate reverse cholesterol transport[35]. Civelek et al. reported no site-specific differences in endothelial ABCA1 expression between susceptible and protected sites of swine arteries[36]. However, our published work showed that ABCA1 level is lower in the mouse aortic arch compared with thoracic aorta[35]. The possible reason for the discrepancy is the different species and diet used in the two studies. Given hypercholesterolemia significantly increased ABCA1 expression in swine endothelium, it might be difficult to detect a site-specific difference of endothelial ABCA1 expression.

The intra- and extra-cellular levels of sterols intricately regulate SREBP2, which in turn modulates cellular cholesterol homeostasis[4]. Significantly, excessive amounts of 25-HC do not prevent OS induction of SREBP2 (Figure 1G), suggesting that the mechano-transduction mechanism overrides that of the cholesterol sensing system, leading to sustained SREBP2 activation. Thus, the disturbed flow-activated SREBP2 appears to disrupt cholesterol homeostasis in its activation of inflammasome. This argument can explain the synergism between atheroprone flow and hyperlipidemia in inducing atherosclerosis.

The ER stress/unfolded protein response (UPR) is activated in EC by atheroprone flow in vitro[37] and is up-regulated in endothelium of swine atheroprone sites *in vivo*[38]. We have previously shown that the UPR chaperone ATF6 inhibits SREBP2 activity by binding to SREBP2 in liver cells under glucose deprivation[14]. This inhibitory effect does not involve ATF6 regulation of SREBP2 maturation, ie, cleavage. In contrast, OS affects SREBP2 cleavage (Figure 1A). Support for the two distinct mechanisms of SREBP2 regulation comes from experiments showing that ATF6 and SREBP2 were co-induced in ECs under OS and ATF6 knockdown by siRNA did not affect SREBP2 induction by OS (data not shown).

Among mechano-sensitive signaling molecules, Akt and AMPK regulate the endothelial phenotypic changes responding to atheroprone and atheroprotective flow, respectively[39]. Akt positively regulates SREBP[40] through direct phosphorylation and transcriptional activation via mTORC1. On the other hand, AMPK inhibits SREBP-1c and -2 activities through Ser372 phosphorylation, which inhibits SREBP cleavage, nuclear translocation, and transcriptional activity[41]. Thus, the disturbed flow-activated Akt is likely involved in SREBP2 activation in atheroprone areas, whereas SREBP2 suppression in atheroresistant areas is at least in part mediated by AMPK. Thus, AMPK activators such as statin and metformin may play the similar beneficial role as that of atheroprotective flow in phosphorylating SREBP2.

SREBP-1a is involved in the lipopolysaccharide (LPS)-stimulated IL-1β production through activation of NLRP1a inflammasome in macrophages[19]. The *SREBP1* promoter region also contains an SRE binding site, which can be regulated by SREBP2[42]. The OS-induced SREBP2 should also activate SREBP1, because ECs transfected with Ad-SREBP2(N) showed an increased expression of SREBP1 (Figure S8). However, we did not find increased levels of NLRP1a in ECs from EC-SREBP2(N)-Tg mice (Figure S8). Most, if not all, NLRP3 activators up-regulate NOXs, with concurrent elevation of the short-lived ROS, so NOX-mediated redox signaling is involved in NLRP3 inflammasome activation[20, 21]. Nevertheless, NOXs are not necessary for inflammasome activation in hematopoietic cells, because immune cells deficient in NOXs show normal or hyperactive activation of inflammasome[43, 44]. In contrast, our data in Figure 3 suggest that SREBP2 transactivation of NOX2 is necessary for inducing NLRP3 inflammasome in ECs. Although the molecular basis of the discrepancies between macrophages and ECs remains unknown, SREBP2 induction of NOX2 is implicated in endothelial biology in that the major enzymatic product of NOX2 is ROS[45].

Summarized in Figure 8, we demonstrated that atheroprone flow, like endogenous damage- and pathogen-associated molecules such as cholesterol crystals and LPS, induces NLRP3 inflammasome in endothelium via SREBP2 activation. This increased innate immunity in endothelium synergizes with hyperlipidemia to result in the focal nature of atherosclerosis.

Supplementary Material

Refer to Web version on PubMed Central for supplementary material.

Acknowledgments

Funding Sources: This work was supported in part by National Institutes of Health Grants HL89940 and HL105318 and National Natural Science Foundation of China 81270349.

References

1. Ross R. Mechanisms of disease - Atherosclerosis - An inflammatory disease. N. Engl. J. Med. 1999; 340:115–126. [PubMed: 9887164]
2. Chiu JJ, Chien S. Effects of disturbed flow on vascular endothelium: pathophysiological basis and clinical perspectives. Physiol. Rev. 2011; 91:327–387. [PubMed: 21248169]
3. Davies PF. Hemodynamic shear stress and the endothelium in cardiovascular pathophysiology. Nat. Clin. Pract. Cardiovasc. Med. 2009; 6:16–26. [PubMed: 19029993]
4. Espenshade PJ, Hughes AL. Regulation of sterol synthesis in eukaryotes. Annu. Rev. Genet. 2007; 41:401–427. [PubMed: 17666007]
5. Najafi-Shoushtari SH, Kristo F, Li Y, Shioda T, Cohen DE, Gerszten RE, Naar AM. MicroRNA-33 and the SREBP host genes cooperate to control cholesterol homeostasis. Science. 2010; 328:1566–1569. [PubMed: 20466882]
6. Rayner KJ, Suarez Y, Davalos A, Parathath S, Fitzgerald ML, Tamehiro N, Fisher EA, Moore KJ, Fernandez-Hernando C. MiR-33 contributes to the regulation of cholesterol homeostasis. Science. 2010; 328:1570–1573. [PubMed: 20466885]
7. Liu Y, Chen BP, Lu M, Zhu Y, Stemerman MB, Chien S, Shyy JY. Shear stress activation of SREBP1 in endothelial cells is mediated by integrins. Arterioscler. Thromb. Vasc. Biol. 2002; 22:76–81. [PubMed: 11788464]
8. Wen H, Ting JP, O'Neill LA. A role for the NLRP3 inflammasome in metabolic diseases--did Warburg miss inflammation? Nat. Immunol. 2012; 13:352–357. [PubMed: 22430788]
9. Duewell P, Kono H, Rayner KJ, Sirois CM, Vladimer G, Bauernfeind FG, Abela GS, Franchi L, Nunez G, Schnurr M, Espevik T, Lien E, Fitzgerald KA, Rock KL, Moore KJ, Wright SD, Hornung

V, Latz E. NLRP3 inflammasomes are required for atherogenesis and activated by cholesterol crystals. Nature. 2010; 464:1357–1361. [PubMed: 20428172]

10. Rajamaki K, Lappalainen J, Oorni K, Valimaki E, Matikainen S, Kovanen PT, Eklund KK. Cholesterol crystals activate the NLRP3 inflammasome in human macrophages: a novel link between cholesterol metabolism and inflammation. PLoS. One. 2010; 5:e11765. [PubMed: 20668705]
11. Hwang J, Ing MH, Salazar A, Lassegue B, Griendling K, Navab M, Sevanian A, Hsiai TK. Pulsatile versus oscillatory shear stress regulates NADPH oxidase subunit expression: implication for native LDL oxidation. Circ. Res. 2003; 93:1225–1232. [PubMed: 14593003]
12. Lim YC, Luscinskas FW. Isolation and culture of murine heart and lung endothelial cells for in vitro model systems. Methods. Mol. Biol. 2006; 341:141–154. [PubMed: 16799196]
13. Zhang Y, Lee TS, Kolb EM, Sun K, Lu X, Sladek FM, Kassab GS, Garland T Jr, Shyy JY. AMP-activated protein kinase is involved in endothelial NO synthase activation in response to shear stress. Arterioscler. Thromb. Vasc. Biol. 2006; 26:1281–1287. [PubMed: 16601232]
14. Zeng L, Lu M, Mori K, Luo S, Lee AS, Zhu Y, Shyy JY. ATF6 modulates SREBP2-mediated lipogenesis. EMBO. J. 2004; 23:950–958. [PubMed: 14765107]
15. Wingender E, Karas H, Knuppel R. TRANSFAC database as a bridge between sequence data libraries and biological function. Pac. Symp. Biocomput. 1997:477–485. [PubMed: 9390316]
16. Ni ZF, Ng DW, Liu JX, Chen ZJ. Chromatin immunoprecipitation (ChIP) assay. Protocol. Exchange. 2009
17. Nakano K, Egashira K, Ohtani K, Gang Z, Iwata E, Miyagawa M, Sunagawa K. Azelnidipine has anti-atherosclerotic effects independent of its blood pressure-lowering actions in monkeys and mice. Atherosclerosis. 2008; 196:172–179. [PubMed: 17481639]
18. Nigro P, Abe J, Berk BC. Flow shear stress and atherosclerosis: a matter of site specificity. Antioxid. Redox. Signal. 2011; 15:1405–1414. [PubMed: 21050140]
19. Im SS, Yousef L, Blaschitz C, Liu JZ, Edwards RA, Young SG, Raffatellu M, Osborne TF. Linking lipid metabolism to the innate immune response in macrophages through sterol regulatory element binding protein-1a. Cell. Metab. 2011; 13:540–549. [PubMed: 21531336]
20. Dostert C, Petrilli V, Van Bruggen R, Steele C, Mossman BT, Tschopp J. Innate immune activation through Nalp3 inflammasome sensing of asbestos and silica. Science. 2008; 320:674–677. [PubMed: 18403674]
21. Zhou R, Tardivel A, Thorens B, Choi I, Tschopp J. Thioredoxin-interacting protein links oxidative stress to inflammasome activation. Nat. Immunol. 2010; 11:136–140. [PubMed: 20023662]
22. Matlung HL, Bakker EN, VanBavel E. Shear stress, reactive oxygen species, and arterial structure and function. Antioxid. Redox. Signal. 2009; 11:1699–1709. [PubMed: 19186981]
23. Suo J, Ferrara DE, Sorescu D, Guldberg RE, Taylor WR, Giddens DP. Hemodynamic shear stresses in mouse aortas: implications for atherogenesis. Arterioscler. Thromb. Vasc. Biol. 2007; 27:346–351. [PubMed: 17122449]
24. Hajra L, Evans AI, Chen M, Hyduk SJ, Collins T, Cybulsky MI. The NF-kappa B signal transduction pathway in aortic endothelial cells is primed for activation in regions predisposed to atherosclerotic lesion formation. Proc. Natl. Acad. Sci. USA. 2000; 97:9052–9057. [PubMed: 10922059]
25. Landmesser U, Hornig B, Drexler H. Endothelial function: a critical determinant in atherosclerosis? Circulation. 2004; 109:II27–II33. [PubMed: 15173060]
26. McGill HC Jr, McMahan CA, Herderick EE, Tracy RE, Malcom GT, Zieske AW, Strong JP. Effects of coronary heart disease risk factors on atherosclerosis of selected regions of the aorta and right coronary artery. PDAY Research Group. Pathobiological Determinants of Atherosclerosis in Youth. Arterioscler. Thromb. Vasc. Biol. 2000; 20:836–845. [PubMed: 10712411]
27. McGill HC Jr, McMahan CA, Gidding SS. Preventing heart disease in the 21st century: implications of the Pathobiological Determinants of Atherosclerosis in Youth (PDAY) study. Circulation. 2008; 117:1216–1227. [PubMed: 18316498]
28. Fearon WF, Fearon DT. Inflammation and cardiovascular disease: role of the interleukin-1 receptor antagonist. Circulation. 2008; 117:2577–2579. [PubMed: 18490534]

29. Chamberlain J, Evans D, King A, Dewberry R, Dower S, Crossman D, Francis S. Interleukin-1beta and signaling of interleukin-1 in vascular wall and circulating cells modulates the extent of neointima formation in mice. Am. J. Pathol. 2006; 168:1396–1403. [PubMed: 16565512]
30. Kirii H, Niwa T, Yamada Y, Wada H, Saito K, Iwakura Y, Asano M, Moriwaki H, Seishima M. Lack of interleukin-1beta decreases the severity of atherosclerosis in ApoE-deficient mice. Arterioscler. Thromb. Vasc. Biol. 2003; 23:656–660. [PubMed: 12615675]
31. Devlin CM, Kuriakose G, Hirsch E, Tabas I. Genetic alterations of IL-1 receptor antagonist in mice affect plasma cholesterol level and foam cell lesion size. Proc. Natl. Acad. Sci. USA. 2002; 99:6280–6285. [PubMed: 11983917]
32. Ridker PM, Thuren T, Zalewski A, Libby P. Interleukin-1beta inhibition and the prevention of recurrent cardiovascular events: rationale and design of the Canakinumab Anti-inflammatory Thrombosis Outcomes Study (CANTOS). Am. Heart. J. 2011; 162:597–605. [PubMed: 21982649]
33. Rayner KJ, Sheedy FJ, Esau CC, Hussain FN, Temel RE, Parathath S, van Gils JM, Rayner AJ, Chang AN, Suarez Y, Fernandez-Hernando C, Fisher EA, Moore KJ. Antagonism of miR-33 in mice promotes reverse cholesterol transport and regression of atherosclerosis. J. Clin. Invest. 2011; 121:2921–2931. [PubMed: 21646721]
34. Rayner KJ, Esau CC, Hussain FN, McDaniel AL, Marshall SM, van Gils JM, Ray TD, Sheedy FJ, Goedeke L, Liu X, Khatsenko OG, Kaimal V, Lees CJ, Fernandez-Hernando C, Fisher EA, Temel RE, Moore KJ. Inhibition of miR-33a/b in non-human primates raises plasma HDL and lowers VLDL triglycerides. Nature. 2011; 478:404–407. [PubMed: 22012398]
35. Zhu M, Fu Y, Hou Y, Wang N, Guan Y, Tang C, Shyy JY, Zhu Y. Laminar shear stress regulates liver X receptor in vascular endothelial cells. Arterioscler. Thromb. Vasc. Biol. 2008; 28:527–533. [PubMed: 18096827]
36. Civelek M, Grant GR, Irolla CR, Shi C, Riley RJ, Chiesa OA, Stoeckert CJ Jr, Karanian JW, Pritchard WF, Davies PF. Prelesional arterial endothelial phenotypes in hypercholesterolemia: universal ABCA1 upregulation contrasts with region-specific gene expression in vivo. Am J Physiol Heart Circ Physiol. 2010; 298:H163–H170. [PubMed: 19897713]
37. Feaver RE, Hastings NE, Pryor A, Blackman BR. GRP78 upregulation by atheroprone shear stress via p38-, alpha2beta1-dependent mechanism in endothelial cells. Arterioscler Thromb Vasc Biol. 2008; 28:1534–1541. [PubMed: 18556570]
38. Civelek M, Manduchi E, Riley RJ, Stoeckert CJ Jr, Davies PF. Chronic endoplasmic reticulum stress activates unfolded protein response in arterial endothelium in regions of susceptibility to atherosclerosis. Circ Res. 2009; 105:453–461. [PubMed: 19661457]
39. Guo D, Chien S, Shyy JY. Regulation of endothelial cell cycle by laminar versus oscillatory flow: distinct modes of interactions of AMP-activated protein kinase and Akt pathways. Circ. Res. 2007; 100:564–571. [PubMed: 17272808]
40. Krycer JR, Sharpe LJ, Luu W, Brown AJ. The Akt-SREBP nexus: cell signaling meets lipid metabolism. Trends. Endocrinol. Metab. 2010; 21:268–276. [PubMed: 20117946]
41. Li Y, Xu S, Mihaylova MM, Zheng B, Hou X, Jiang B, Park O, Luo Z, Lefai E, Shyy JY, Gao B, Wierzbicki M, Verbeuren TJ, Shaw RJ, Cohen RA, Zang M. AMPK phosphorylates and inhibits SREBP activity to attenuate hepatic steatosis and atherosclerosis in diet-induced insulin-resistant mice. Cell. Metab. 2011; 13:376–388. [PubMed: 21459323]
42. Amemiya-Kudo M, Shimano H, Yoshikawa T, Yahagi N, Hasty AH, Okazaki H, Tamura Y, Shionoiri F, Iizuka Y, Ohashi K, Osuga J, Harada K, Gotoda T, Sato R, Kimura S, Ishibashi S, Yamada N. Promoter analysis of the mouse sterol regulatory element-binding protein-1c gene. J. Biol. Chem. 2000; 275:31078–31085. [PubMed: 10918064]
43. Meissner F, Seger RA, Moshous D, Fischer A, Reichenbach J, Zychlinsky A. Inflammasome activation in NADPH oxidase defective mononuclear phagocytes from patients with chronic granulomatous disease. Blood. 2010; 116:1570–1573. [PubMed: 20495074]
44. van de Veerdonk FL, Smeekens SP, Joosten LA, Kullberg BJ, Dinarello CA, van der Meer JW, Netea MG. Reactive oxygen species-independent activation of the IL-1beta inflammasome in cells from patients with chronic granulomatous disease. Proc. Natl. Acad. Sci. USA. 2010; 107:3030–3033. [PubMed: 20133696]

45. Takac I, Schroder K, Brandes RP. The Nox family of NADPH oxidases: friend or foe of the vascular system? Curr Hypertens Rep. 2012; 14:70–78. [PubMed: 22071588]

Clinical Perspective

Atherosclerosis preferentially develops at branches and curvatures in the arterial tree and disturbed flow pattern imposed in the endothelium in these regions play a major role in the preferentially localized atherosclerosis. In this study, we show that disturbed flow increases endothelial innate immunity via NLRP3 inflammasome in vitro and in vivo. The underlying mechanism involves the induction of sterol regulatory element binding protein 2 (SREBP2) which transactivates NADPH oxidase 2 (NOX2) and NLRP3. The increased innate immunity in endothelium predisposes hyperlipidemia to result in the focal nature of atherosclerosis. This newly defined SREBP2/NLRP3 inflammasome pathway suggests that SREBP2 could be a therapeutic target to prevent atherosclerosis initiation, which is in line with the anti-atherosclerosis effect of IL-1β antagonism.

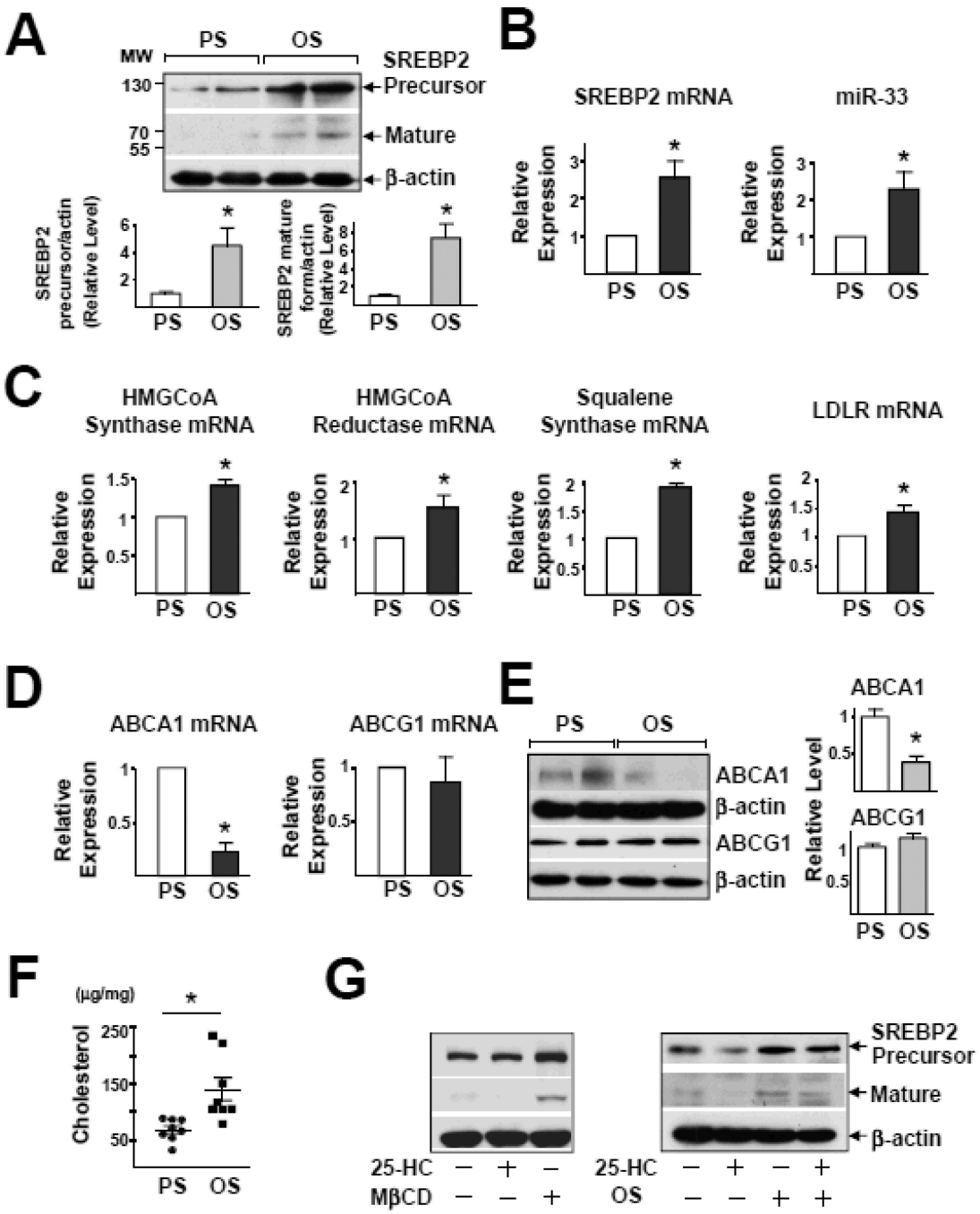

Figure 1.

OS Induces SREBP2 and miR-33 in HUVECs. HUVECs were exposed to a PS, (12 ± 4 dyn/cm^2) or OS (1 ± 4 dyn/cm^2) for 14 hr. (**A**) Representative immunoblot for precursor SREBP2 and mature form of SREBP2. (**B**) Analysis of levels of SREBP2 mRNA and miR-33 by RT-PCR. (**C**) The mRNA levels of HMG-CoA synthase, HMG-CoA reductase, squalene synthase, and LDLR. (**D**) The mRNA levels of ABCA1 and ABCG1. (**E**) Representative immunoblot for ABCA1 and ABCG1. (**F**) Total cellular cholesterol level (n = 8). (**G**) Representative immunoblot for precursor SREBP2 and mature form of SREBP2 in HUVECs treated with MβCD, 25-HC (1 μg/mL), or OS plus 25-HC (1 μg/mL). Data are

mean ± SEM from at least 3 independent experiments. Student's *t* test or Mann-Whitney U test with exact method was used. '*' indicates $p < 0.05$.

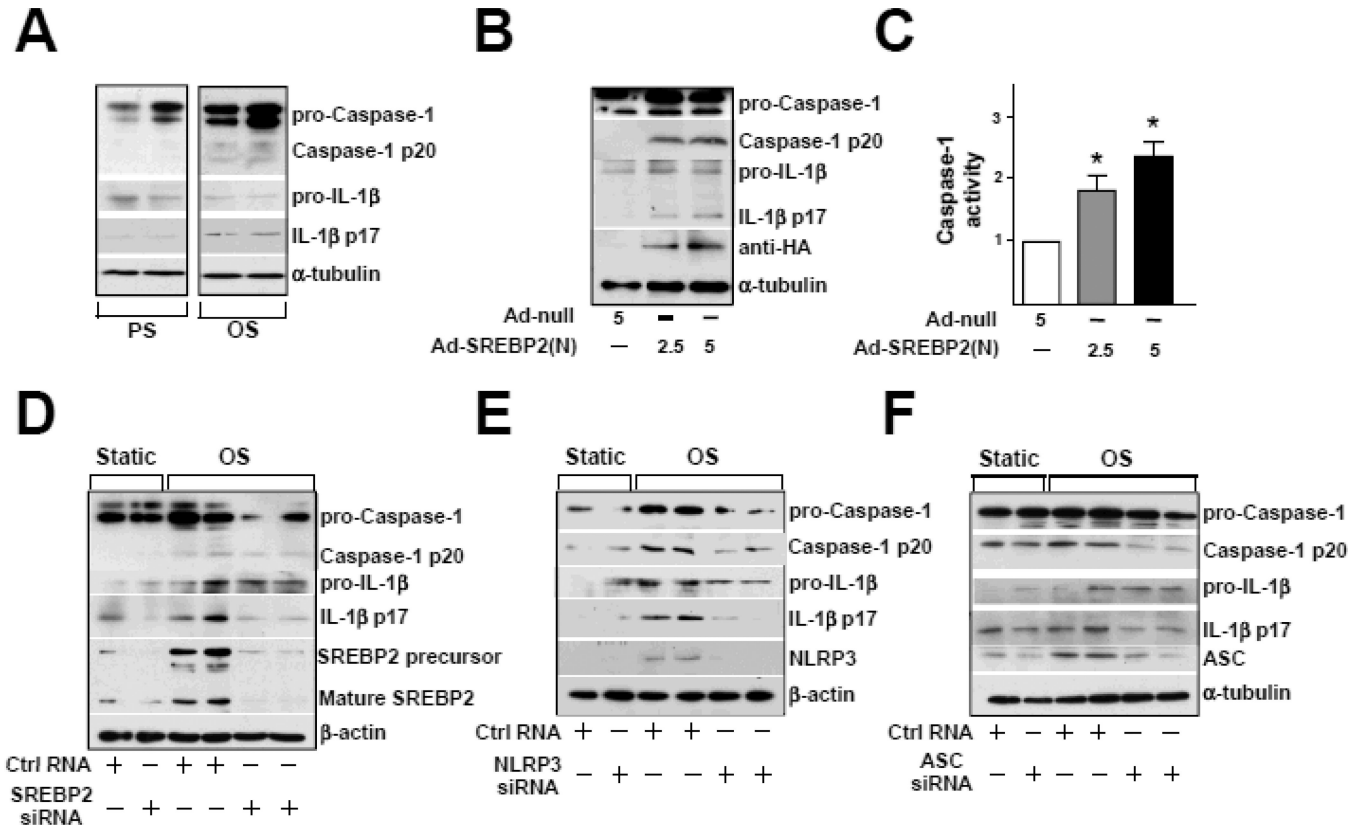

Figure 2.

OS Induces NLRP3 Inflammasomes in ECs via SREBP2. (**A**) Representative immunoblot for pro-caspase-1, caspase-1 p20, pro-IL-1β, and IL-1β p17 in HUVECs exposed to PS or OS for 14 hr and (**B**) in HUVECs treated with Adenovirus-null (Ad-null, 5 MOI), Adenovirus-SREBP2(N) tagged with HA [Ad-SREBP2(N), 2.5 MOI or 5 MOI]. (**C**) Caspase-1 activity of extracts from HUVECs treated with Ad-null, 5 MOI, Ad-SREBP2(N), 2.5 MOI or 5 MOI. Data are mean ± SEM normalized to Ad-null group for each independent experiment. Mann-Whitney U test with exact method was used. $*p < 0.05$ compared with Ad-null. (**D**) Representative immunoblot of pro-caspase-1, caspase-1 p20, pro-IL-1β, IL-1β p17, SREBP2 precursor, and mature form of SREBP2 in HUVECs transfected with 20 nM control RNA or SREBP2 siRNA for 48 hr, then exposed to static conditions or OS for 14 hr. (**E**) Representative immunoblot for pro-caspase-1, caspase-1 p20, pro-IL-1β, IL-1β p17, and NLPR3 in HUVECs transfected with 20 nM control RNA or NLRP3 siRNA for 48 hr, then exposed to static conditions or OS for 14 hr. (**F**) Representative immunoblot of pro-caspase-1, caspase-1 p20, pro-IL-1β, IL-1β p17, and ASC in HUVECs transfected with 20 nM control RNA or ASC siRNA for 48 hr, then exposed to static conditions or OS for 14 hr.

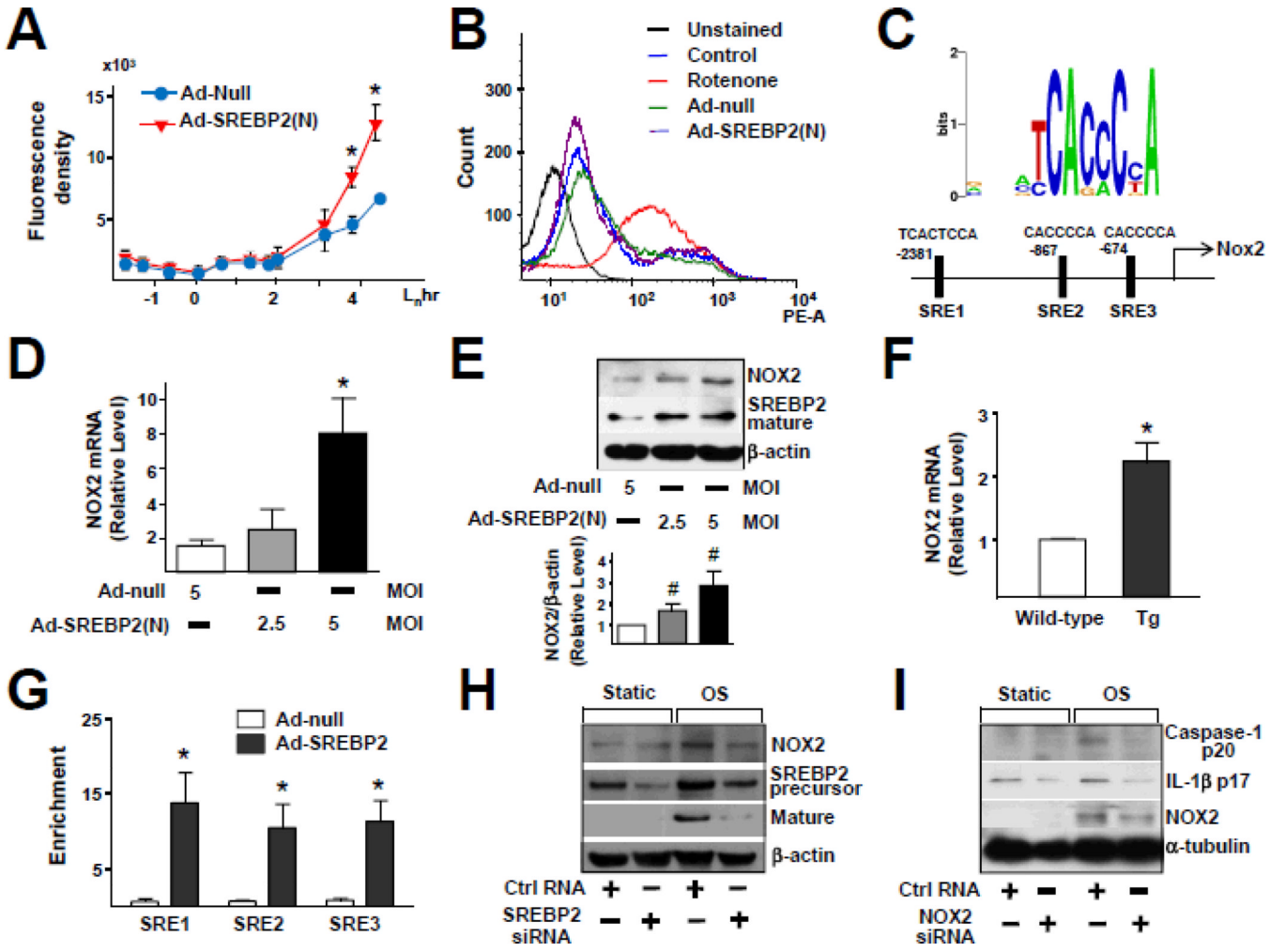

Figure 3.

SREBP2 Up-regulates NOX2 with Attendant Increase in ROS in ECs. (**A**) ROS production monitored by measuring H2DCFDA fluorescence in HUVECs infected with Ad-null or Ad-SREBP2(N) (5 MOI). (**B**) Cytometric analysis of HUVECs infected with Ad-null or Ad-SREBP2(N) (5 MOI) for 48 hr or treated with rotenone (40 μM) for 3 hr and then stained with MitoSOX for 30 min. (**C**) Depiction of the 3 putative SRE binding sites, at −2381/−2367(SRE1), −867/−861(SRE2), and −674/668(SRE3) bp upstream of the transcription initiation site in the human *NOX2* promoter. NOX2 mRNA levels (**D**) and representative immunoblot (and quantification) of NOX2 and the cleaved SREBP2 (**E**) in HUVECs treated with Ad-null (5 MOI) or Ad-SREBP2(N) (2.5 MOI or 5 MOI). (**F**) NOX2 mRNA levels in lung ECs from wild-type or EC-SREBP2(N)-Tg mice (n = 8). (**G**) ChIP analysis with antibodies against SREBP2 or IgG, soluble chromatin (~500 bp in length) from HUVECs infected with Ad-null or Ad-SREBP2(N), and primers targeting the region spanning the 3 SRE binding sites in the *NOX2* promoter. (**H**) Representative immunoblot of NOX2, SREBP2 precursor and mature form of SREBP2 in HUVECs transfected with 20 nM control RNA or SREBP2 siRNA for 48 hr, then exposed to static or OS for 14 hr. (**I**) Representative immunoblot of caspase-1 p20, IL-1β p17, and NOX2 in HUVECs transfected with 20 nM control RNA or NOX2 siRNA for 48 hr, then exposed to static or OS for 14 hr. At least 3 independent experiments were performed and results are mean ± SEM. Mann-

Whitney U test with exact method was used. '*' indicates $p < 0.05$ vs Ad-null or wild-type. '#' indicates $p = 0.05$.

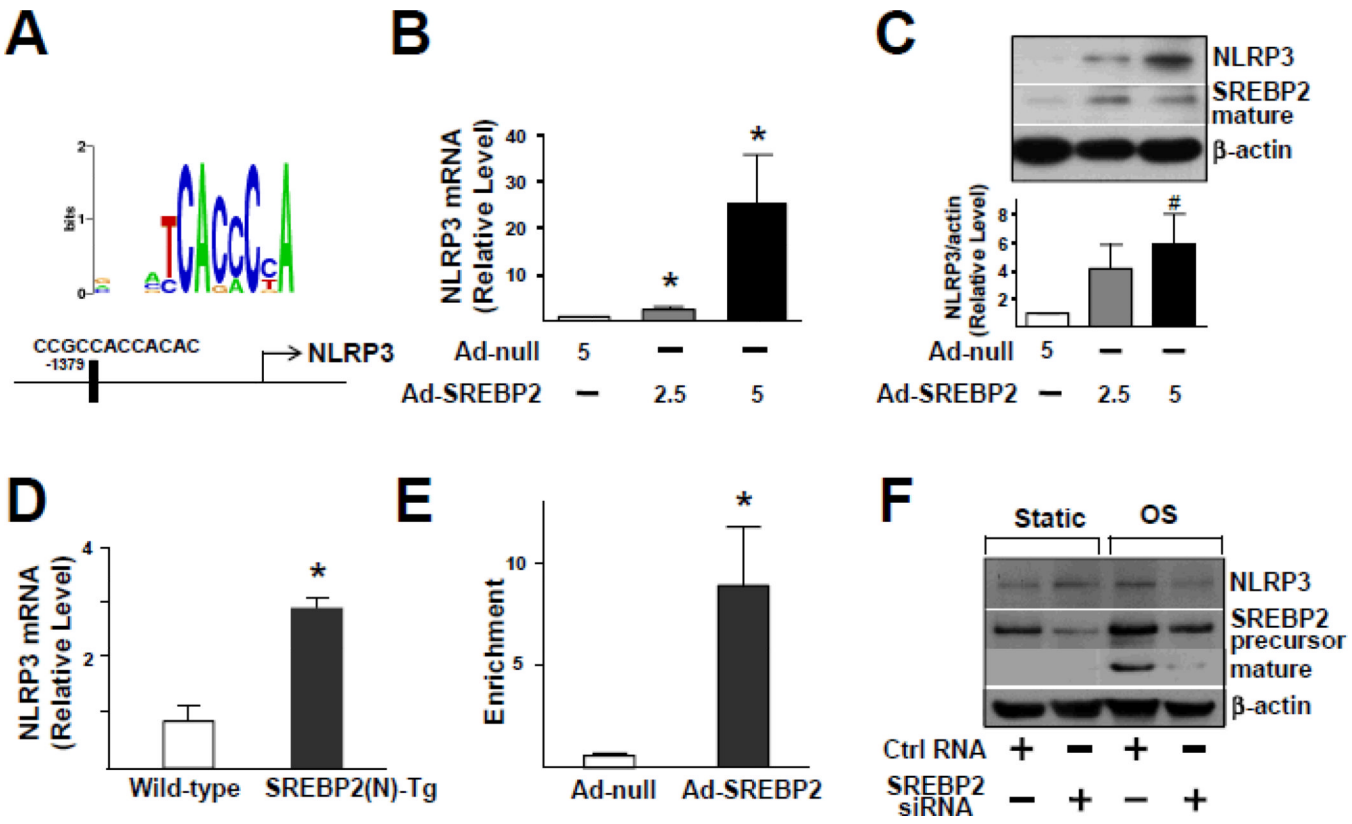

Figure 4.

SREBP2 Overexpression Up-regulates NLRP3 Inflammasome. (**A**) Depiction of the putative SRE binding site located at −1379/−1368 bp upstream of the transcription initiation site in the human NLRP3 promoter. The NLRP3 mRNA levels (**B**) and representative immunoblot (and quantification) of NLRP3 and the mature form of SREBP2 (**C**) in HUVECs treated with Ad-null (5MOI), Ad-SREBP2(N) (2.5 MOI or 5 MOI). (**D**) NLRP3 mRNA levels in lung ECs from wild-type or EC-SREBP2(N)-Tg mice (n=8). (**E**) ChIP analysis with antibodies against SREBP2 or IgG, soluble chromatin from HUVECs infected with Ad-null or Ad-SREBP2(N), and primers targeting the region spanning the SRE binding site in the *NLRP3* promoter. (**F**) Representative immunoblot of NLRP3, precursor SREBP2, and mature form of SREBP2 in HUVECs transfected with 20 nM control RNA or SREBP2 siRNA for 48 hr, then exposed to static conditions or OS for 14 hr. Bar graphs represent mean ± SEM from at least 3 independent experiments. Mann-Whitney U test with exact method was used. '*' indicates $p < 0.05$ vs Ad-null or wild-type whereas '#' indicates $p = 0.05$ vs Ad-null.

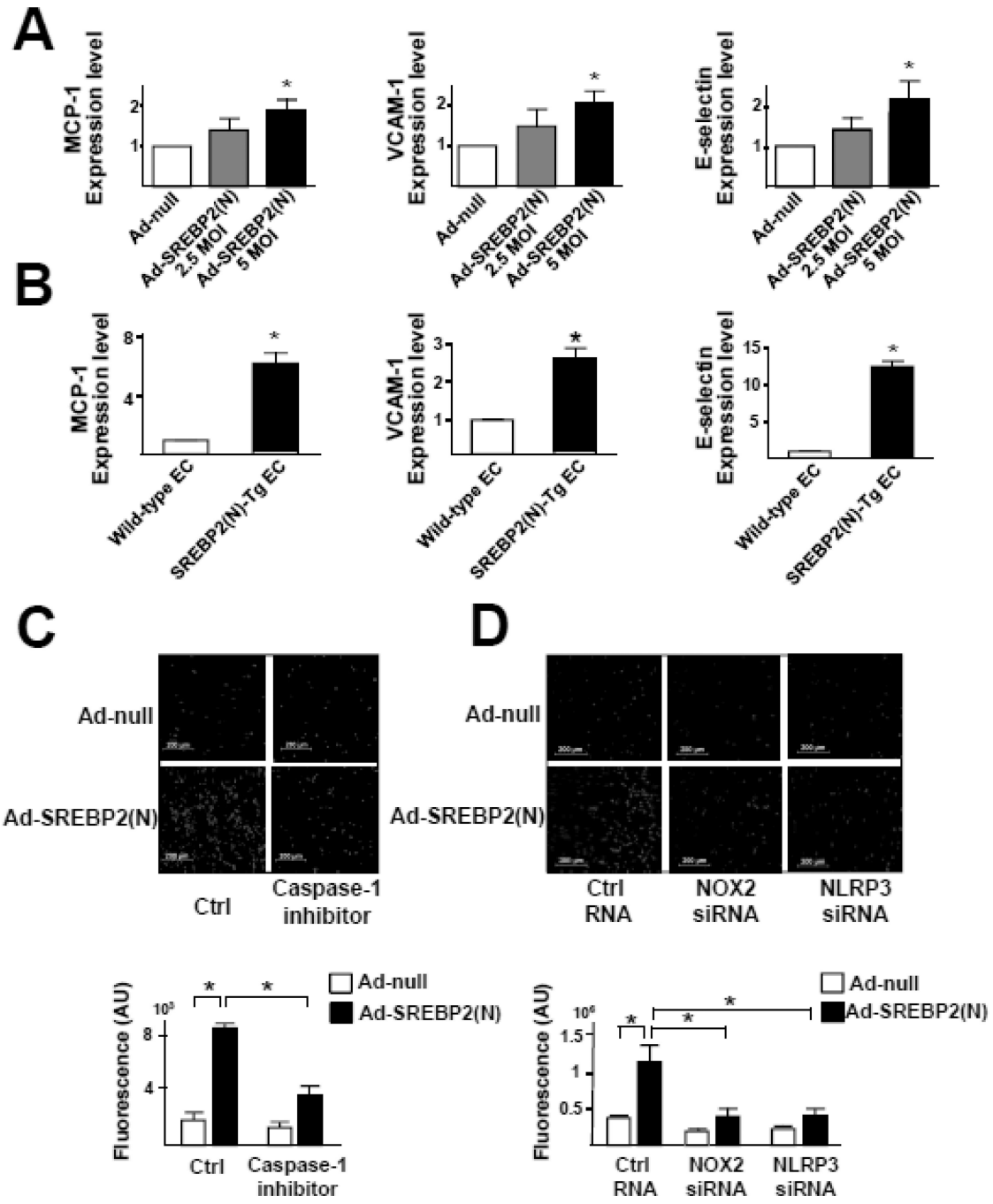

Figure 5.

Increased Level of SREBP2 Causes EC NLRP3 Inflammation. (**A**) Quantification of mRNA levels of MCP-1, VCAM-1, and E-selectin in HUVECs treated with Ad-null (5 MOI) or Ad-SREBP2(N) (2.5 or 5 MOI) or (**B**) in lung ECs from wild-type or EC-SREBP2(N)-Tg mice (n = 8). (**C,D**) HUVECs were infected with Ad-null or Ad-HA-SREBP2(N) for 24 hr, then treated with or without caspase-1 inhibitor Z-YVAD-FMK (2 μM) for 24 hr. In separate experiments, HUVECs were transfected with control RNA, NOX2 siRNA, or NLRP3 siRNA, then infected with Ad-null or Ad-HA-SREBP2(N) for 24 hr. The cells were incubated for 30 min with LeukoTracker™-labeled THP1 cells. For quantification, parallel

batches of treated cells were lysed and the fluorescence measured. Data are mean ± SEM from 3 independent experiments performed in triplicate. Mann-Whitney U test with exact method was used and '*' indicates $p < 0.05$ for comparisons with Ad-null or wild- type ECs.

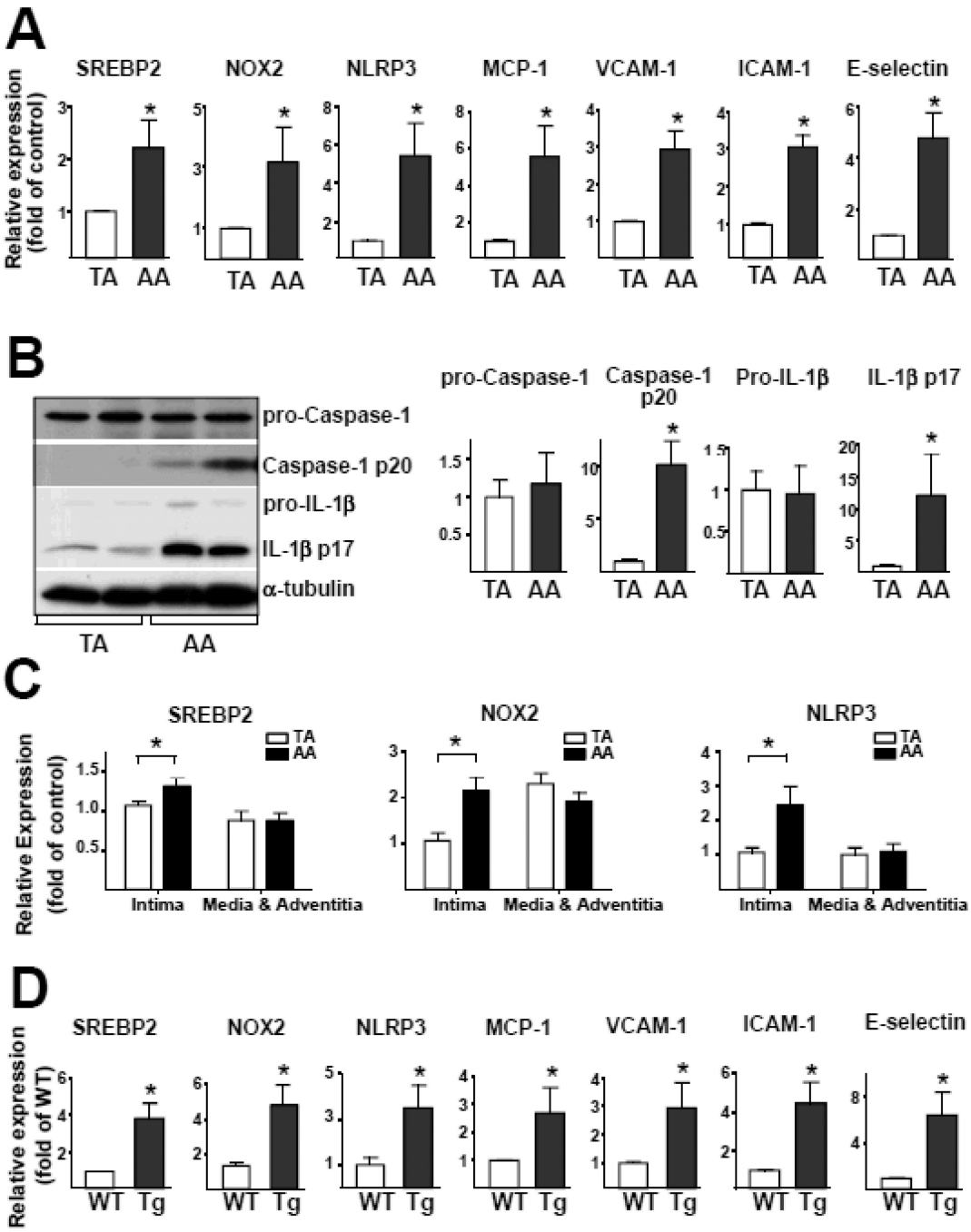

Figure 6.

SREBP2-NOX2-inflammasome Activation in Atheroprone Regions of Mouse Aortas. (**A**) Quantification of mRNA levels of SREBP2, NOX2, NLRP3, MCP-1, VCAM-1, ICAM-1, and E-selectin in the thoracic aorta (TA) and aortic arch (AA) of C57BL/6 mice (n = 7). (**B**) Representative immunoblot of pro-caspase-1, caspase-1 p20, pro-IL-1β, and IL-1β p17 in TA and AA from C57BL/6 mice. (**C**) The level of SREBP2, NOX2 and NLRP3 mRNA in aortic intima or media and adventitia. Data are mean ± SEM of the relative mRNA normalized to that of β-actin (n = 18). (**D**) Quantification of mRNA levels of SREBP2, NOX2, NLRP3, MCP-1, VCAM-1, ICAM-1, and E-selectin in TA from wild-type (n = 7)

and EC-SREBP2(N)-Tg mice (n = 7). Mann-Whitney U test with exact method was used. '*' indicates $p < 0.05$ for comparisons with TA or WT.

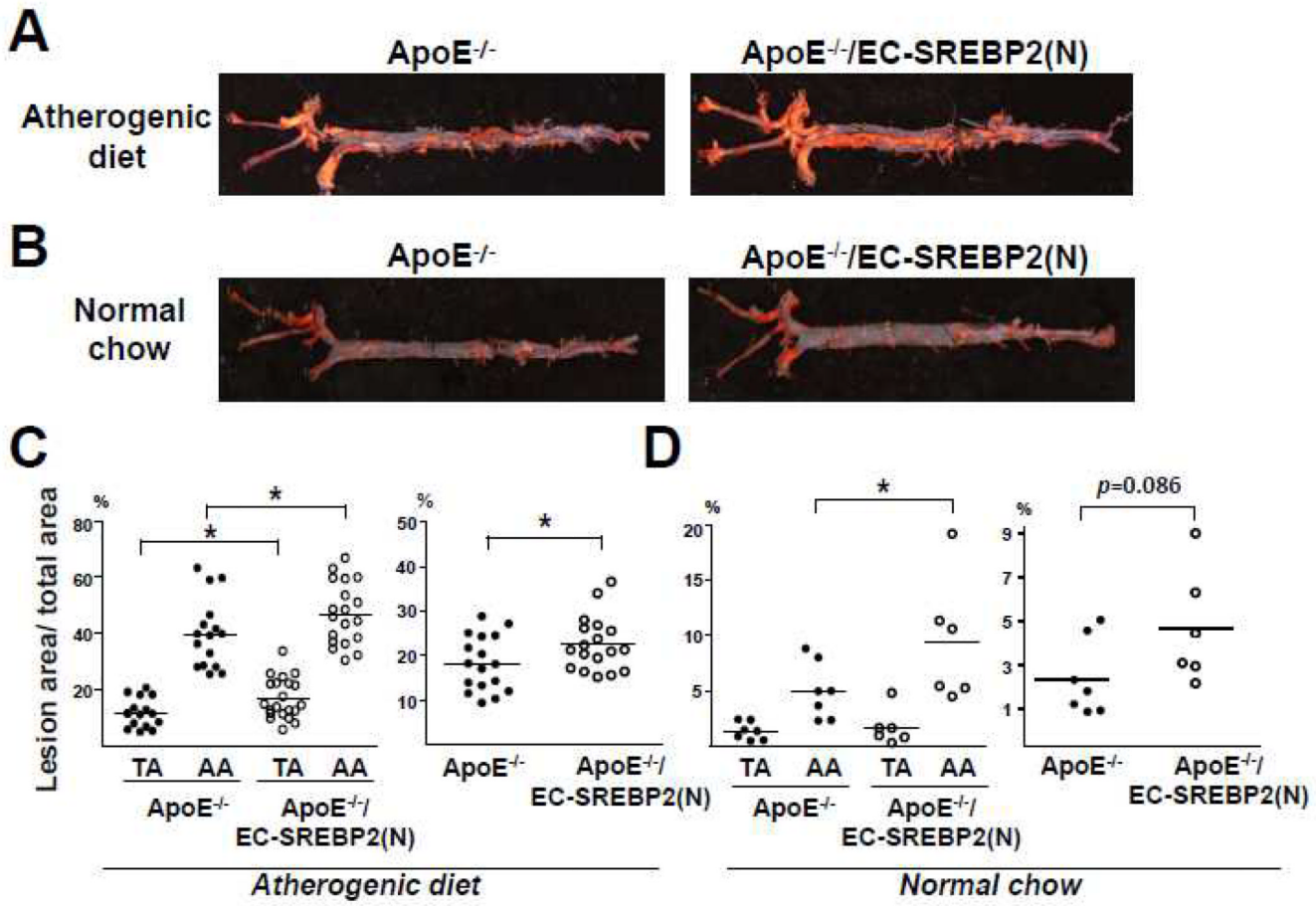

Figure 7.

Overexpression of SREBP2 in ECs Enhances Atherosclerosis. (**A**) Representative Oil Red O staining of aortas from (**A**) Eight-week-old ApoE$^{-/-}$ (n = 17) and ApoE$^{-/-}$/SREBP2(N) mice (n = 18) fed a high-fat diet for 8 weeks and (**B**) 24-week-old ApoE$^{-/-}$ (n = 7) and ApoE$^{-/-}$/SREBP2(N) mice (n = 6) fed a normal chow. (**C,D**) Quantification of percentage lesion areas in the TA, AA, and whole aorta from groups in **(A)** and **(B)**. Student's *t* test or Mann-Whitney U test with exact method was used. '*' indicates $p < 0.05$.

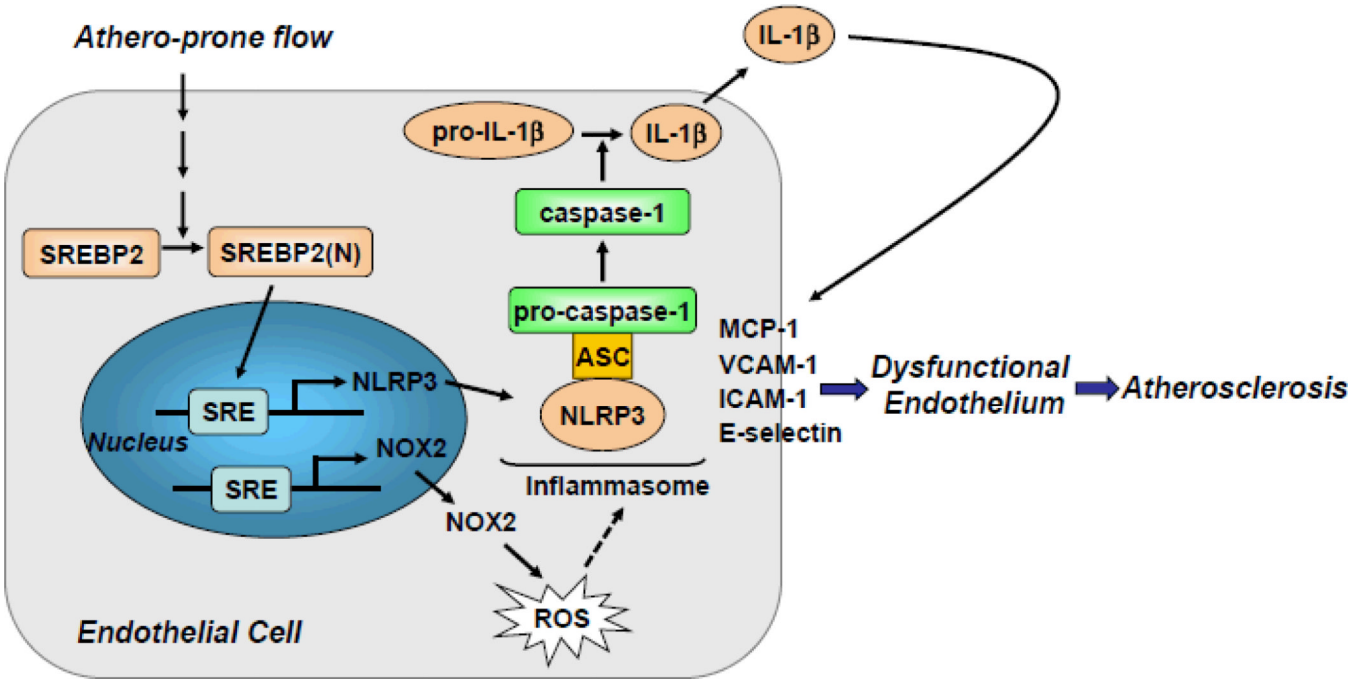

Figure 8.
Graphic Summary for the Mechanism that SREBP2 Activation of NLRP3 Inflammasome in Endothelium Mediates Atheroprone flow-Induced Atherosclerosis.

Table 1

Serum lipid profile of ApoE$^{-/-}$/EC-SREBP2(N) and their ApoE$^{-/-}$ littermates fed a normal chow or atherogenic diet.

Serum Lipids (mg/dL)	Normal Chow*		Atherogenic Diet†	
	ApoE$^{-/-}$(n = 7)	ApoE$^{-/-}$/EC-SREBP2(N) (n = 6)	ApoE$^{-/-}$(n = 17)	ApoE$^{-/-}$/EC-SREBP2(N) (n = 18)
Total cholesterol	1284 ± 272‡	1224 ± 334	1806 ± 298	1967 ± 576
Triglyceride	169 ± 49	197 ± 112	111 ± 57	125 ± 89
LDL	490 ± 54	478 ± 83	1055 ± 168	1035 ± 235
VLDL	30 ± 14	39 ± 22	21 ± 12	29 ± 22
HDL	764 ± 253	707 ± 374	730 ± 177	903 ± 365

*Normal chow group was 24-week old mice fed a normal chow.

†Atherogenic diet group was 8-week old mice fed an atherogenic diet for 8 weeks.

‡All values are expressed as mean ± SD averaged from number of animals as indicated.

Table 2

Serum lipid profile of EC-SREBP2(N) and their wild-type littermates fed an atherogenic diet.

Serum Lipids (mg/dL)	Wild-type (n = 5)	EC-SREBP2(N) (n = 5)
Total cholesterol	161 ± 6 *	176 ± 30
Triglyceride	56 ± 13	59 ± 11
LDL	16 ± 4	12 ± 2
VLDL	105 ± 31	107 ± 20
HDL	62 ± 36	68 ± 20

* All values are expressed as mean ± SD averaged from number of animals as indicated.